Soil Moisture Mapping Using Active Microwave for a Semi-Distributed Hydrologic Model: Case study in Turkey

Ali Unal Sorman[1*] and Musa Yilmaz[2]
[1] Middle East Technical University, Department of Civil Engineering, Ankara, Turkey
sorman@metu.edu.tr, tel no: +90 532 4302612, fax no: +90 312 2107956
[2] Nesma Eser Onur Contracting Co., Turkey, musayilmaz@gmail.com

***Abstract*-- Soil moisture condition of a watershed plays a significant role in separation of rainfall into infiltration and surface runoff, and hence is a key parameter for the majority of physical hydrological models.**

A semi-empirical backscatter (Dubois) model is utilized in the reverse order to develop radar backscatter versus soil roughness relationship and soil roughness maps of the study area are produced. Another relationship is built between radar backscatter and the three governing soil surface parameters as local incidence angle, soil moisture and soil roughness, in order to use in the development of soil moisture estimation.

The soil moisture maps of the basin are then introduced as input to a semi-distributed hydrological model study using, HEC-HMS, as the initial soil moisture condition of a flood event simulation in 2005. A comparison between both the distributed and lumped model simulation results using active microwave images with the observed field data is carried out using statistic parameter, the root mean square error (RMSE). The distributed model runs resulted in RMSE as 0.35 for both radar approaches and lumped model simulation gave a higher value 0.43. The differences in peak flows were ranged between 1-2 % for the distributed case and 9% for the lumped model approach. But the runoff volume differences were in reverse order being less 0.2% for the lumped and changed in between 7.5-7.0% for distributed (SAR and ASAR radar) model applications.

***Index Term*-- Soil moisture, Synthetic Aperture Radar, Hydrologic model, Turkey.**

1. INTRODUCTION

Soil moisture is the water held in the upper soil layer in the root zone. Despite the fact that it constitutes a very small portion of the global water resources, soil moisture is an important surface variable for meteorology, agriculture, hydrology fields. In the scope of engineering hydrology, soil moisture controls the separation of rainfall into infiltration and surface runoff, and excess soil moisture could lead to high floods, where as deficiency of it could lead to droughts.

The remote sensing instruments which operate in the visible and infrared portions of the electromagnetic spectrum can provide limited information about variations in soil moisture. Due to the large difference in dielectric constants of dry soil and water, and sensitivity of the microwave region to surface dielectric properties, microwave remote sensing and particularly the commonly available radars (synthetic, SAR and advanced aperture, ASAR) are potential tools for such studies. Moreover, microwave remote sensing has the advantages of penetrating clouds and independent of the sun as the source of illumination.

2. OBJECTIVES and RELATED STUDIES

The main objective of this research paper is to get areal distributed soil moisture maps of a pilot catchment with microwave remote sensing as an input to semi-distributed hydrologic modeling for runoff hydrograph simulation. A micro catchment located in western Anatolia, Kurukavak basin in Turkey, is selected as the pilot area. Nine field visits are performed to the basin during 2004 – 2005 water years and soil moisture measurements are carried out on 68 locations with a Time Domain Reflectometer (TDR). The field studies are planned in advance to match radar image acquisitions for various soil moisture conditions. Since field measurements of soil surface roughness is not held during field studies, a relationship between radar backscatter and surface roughness was developed as the first objective of this research.

An algorithm for retrieval of soil moisture from radar imagery for bare soil surfaces is introduced as the second step establishing a relationship between radar backscatter and three governing surface parameters namely local incidence angle, soil moisture and soil roughness. Then, surface soil moisture distribution of the catchment is calculated using three different methods. Similar to the analyses held with soil roughness, these methods are first developed with the point measurements of soil moisture and then applied to other areas of the basin by re-sampled kriging technique. The Backscatter Correction (BS) Factors as method I, which does not include vegetation effect on radar backscatter, is built for bare or sparsely vegetated farmland and pasture fields of the basin.

The step three is followed to propose an algorithm that would be used for microwave remote sensing of soil moisture on vegetation covered areas of the basin. For this reason, the second method of soil moisture estimation, a delta index approach combined with the Water Cloud Model (WCM) for the farmland and pasture land use classes under dense vegetation cover condition.

Lastly, the third method called Basin Indexes (BI) is applied for the forested areas of the basin where radar remote sensing of soil moisture is impractical. This method depends only on watershed terrain indexes using the topographic and solar radiation indices. Finally, all these three soil moisture estimation methods are combined together to produce areal soil moisture maps of the whole catchment area on four of the field study out of nine visits. The distributed soil moisture maps of the basin are introduced within a semi-distributed hydrological model. Semi-distributed rainfall-runoff model simulation of the flood event observed on 1st June 2005 is carried out with Hydrologic Engineering Center – Hydrologic Modeling System [7]. In this part of the study, the soil moisture maps of the Kurukavak catchment are introduced as input to the HEC-HMS model at the beginning of the simulation period. In order to question the contribution of distributed initial soil moisture data on model results, simulation of the same flood event is also performed using a lumped initial soil moisture condition for the entire basin. Finally, the semi distributed and lumped model simulation results are compared with the observed flood hydrograph records measured at the basin outlet.

When one looks at the previous studies in the literature on similar topics, they show that there is a possibility of using synthetic aperture radar (SAR) and/or advanced SAR (ASAR) data to monitor surface moisture from space. Some linear relationships have been empirically derived for various land covers. Some of these published works in recent years will be summarized briefly in the following paragraphs.

Soil moisture estimation is done with ERS-1 SAR data in the East-German loess soil area by [19] and the dependency of the radar backscattering coefficient is related to the soil moisture content with a linear relation. This relation was only valid for bare and loamy soils with a roughness height of about 2 cm.

Later on, soil moisture is estimated from ERS/SAR data using operational methodology by [8] using different soil compositions and land cover uses. The methodology is implemented based on two steps; the calibration and operation periods.

Soil moisture is studied using ERS 2 SAR data as a case study in the Solani River being a tributary to the River Gonga in India by [5] in 2004 for bare and vegetative soils in combined manner. Higher values of determination coefficient were obtained using linear correlation between backscattered values with the volumetric soil moisture data.

Assimilation of scatterometer soil moisture data from ERS satellites are also examined for improving hydrologic studies by [12] in 2006. During model calibration stage, the relationship improved for small topographical variability and low vegetation, but the relationship was still poor and assimilation did not change the model efficiency with respect to daily flow.

Intercomparison of RS-Scat and AMRS-E soil moisture observation over France is carried by [14] in 2009 using different platforms to provide soil moisture information in a much larger spatial scale. This methodology cannot be applied for a smaller catchment what we have used in this research in Turkey. The AMSR-E soil moisture product had significant differences when compared to other datasets due to lack of seasonal variability in soil moisture dynamics.

Lately in 2011, an intercomparison of soil moisture estimates are also done by [6] in 2011 using thermal band and passive MW remote sensing. Background of the soil moisture is monitored and the relative error is estimated using spatial, temporal correlation techniques and a triple collocation error estimation method. It is concluded that thermal infrared and MW methods provide complementary information for the soil moisture state over moderate to dense vegetation cover.

3. STUDY AREA AND DATA COLLECTION

The small catchment located within the western part of Turkey with an area of 4.73 km^2, is selected as the study area of this research. The Digital Elevation Model (DEM), obtained from 1/25000 scaled contour maps of the area, and the drainage network map of the basin is presented in Figure 1. The maximum and minimum elevations of the basin ranged from 1080 m to 840 m, respectively. The Kurukavak Basin is one of the pilot basins of General Directorate of Agricultural Research of Turkey (TAGEM) who has been collecting rainfall and runoff data within the basin since 1984.

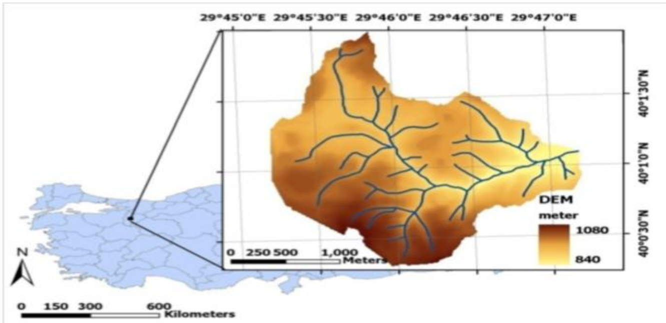

Fig. 1. The DEM and Drainage map of the Kurukavak basin

The land use map of the site obtained from the same organization with geographic locations of field measurement plots is shown in Figure 2, areal distribution of the land use classes is computed (in percentages and in square kilometers) as given in Table I. About half of the basin is covered with forest and the rest of the area is almost shared with two land use classes; farmland and pasture.

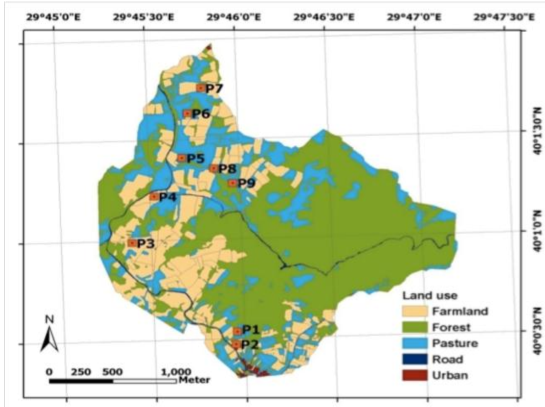

Fig. 2. Land use map of the study site and geographic soil measurement plots

 IJENS

TABLE I
Areal distribution of the land use classes within the basin

Land use	Area (km^2)	Area (%)
Farmland	1.12	23.6
Pasture	1.03	21.9
Forest	2.51	53.1
Other	0.07	1.4

A total of nine field trips were carried out within the basin between September 2004 and August 2005. Soil moisture data records using a Time Domain Reflectometer at the previously selected 68 stationary points were collected and grouped within 9 plots. Since radar waves could not penetrate through dense vegetation canopy such as forest, these measurement locations are selected mostly over farmland and pasture fields of the basin. The geographic locations of these measurement plots are marked in Figure 2. The land use classes and the number of measurement points within each plot are marked. In addition to all 68 plots, the Kriging interpolation technique [16] is applied to increase the number of points to 126. The number of original and re-sampled points within each plot is presented in Table II. As a sample, the original and re-sampled point soil moisture locations for Plot 1 is indicated in Figure 3.

TABLE II
The original number using TDR and resampled points (Kriging) for each plot

Plot	Land use	Number of Points	
		Original - TDR	Resampled - Kriging
P1	Farmland	6	9
P2	Farmland	8	9
P3	Farmland	9	12
P4	Farmland	10	24
P5	Pasture	8	20
P6	Farmland	7	12
P7	Farmland	9	16
P8	Pasture	7	15
P9	Pasture	4	9
Total	6 Farmland + 3 Pasture	68 = 49 + 19	126 = 82 + 44

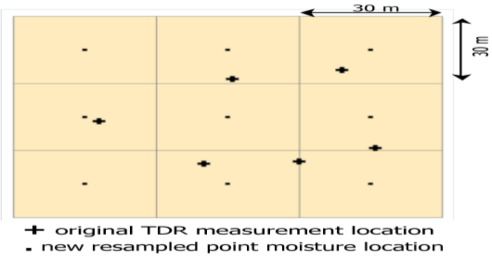

Fig. 3. Original and resampled point soil moisture locations in Plot 1

4. METHODOLOGY FOR PARAMETERIZATION of SOIL CHARACTERISTICS

4.1-Soil Surface Roughness

Soil surface roughness is one of the surface geometric characteristic which has a dominant effect on radar backscatter, intensity of the return signals. In general terms, roughness is a measurement of the small-scale variations in the height of a physical surface. From radar remote sensing point of view, a surface is called as *rough* if it scatters the incoming radar energy in all directions and returns a significant portion back to the antenna. Consequently, a surface is called as *smooth* if it reflects most of the energy away from the antenna [11].

Surface roughness is usually described by two parameters: standard deviation of surface height (**h**) and correlation length (**c**) [18]. The first roughness parameter is also referred as root mean square height of surface variations [15] or simply root mean square roughness and represents the amount of deviations observed over the soil surface from the reference/mean surface. As illustrated in the Figure 4, the root mean square roughness, h, is obtained by measuring the surface variations (r_i) from the reference/mean surface (shown with the dotted line) along a sampling length of L.

In this study, since no field measurement of roughness parameters are available, inversion of the semi-empirical Dubois backscatter model [4], which has a single roughness parameter (root mean square of surface heights; h), is utilized for computation of soil surface roughness on bare fields of the study catchment as shown in Figure 4 and expressed with equation 1.

$$h = \sqrt{\frac{1}{L}\int_0^L r^2(x)\,dx} \qquad (1)$$

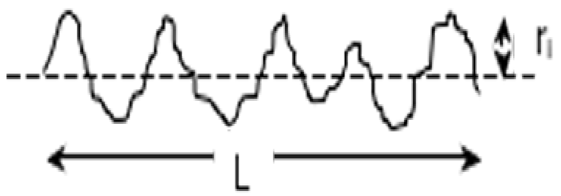

Fig. 4. Soil surface roughness on bare land

4.2-Land use and cover (Vegetation)

Similar to soil surface roughness, vegetation cover of the target area has a significant effect on the radar backscatter. For this purpose, using small wavelengths are more suitable for sensing crops and trees, on the other hand, larger wavelengths are used for sensing trunks and limbs. Moreover, vegetation with higher moisture content returns more signals than that with lower moisture content [11].

4.3-Post-processing of radar imageries

Radar images that are acquired by the AMI of ERS-2 (SAR) and ENVISAT-1 (ASAR) satellites are used during the field campaign. The ASAR instrument on the ENVISAT platform works within the C band of microwave spectrum (5.3 GHz). Different from ERS-2 SAR images which also work within the C band, the ASAR images could be acquired in one of the three polarization modes: HH, VV and VH, and, at a number of incident angles.

In one year time period (between October 2004 and August 2005), a total of nine field studies are performed and a total of 16 SAR and ASAR images are acquired (Table III). Among these field trips and images, four of them; (**09-Oct-2004**, **18-Dec-2004**, **07-May-2005** and **20-Aug-2005)**, are selected for mapping surface soil moisture condition of the basin to represent various soil conditions with land cover. The selection is based on the vegetation condition of the study fields and the number of images acquired on that day. As tabulated in Table III, on the selected field study dates two radar images, SAR and ASAR, are used for analysis

TABLE III

Available radar imagery dates for the study area and average soil moisture

Date	ERS-2 / ENVISAT-1	Time of Acquisition SAR/ASAR UTC	Vegetation Condition for Farmland & Pasture Fields	Average Soil Moisture (%)
09-Oct-2004	SAR/ASAR	8:44/8:16	Sparse	16.17
13-Nov-2004	SAR	8:44	Sparse	13.79
15-Dec-2004	-	-	Almost Bare	27.90
18-Dec-2004	SAR/ASAR	8:44/8:16	Almost Bare	20.50
28-Apr-2005	ASAR	7:59	Dense	24.30
07-May-2005	SAR/ASAR	8:44/8:16	Dense	26.12
02-Jun-2005	ASAR	7:59	Dense	34.40
11-Jun-2005	SAR/ASAR	8:44/8:16	Dense	29.24
20-Aug-2005	SAR/ASAR	8:44/8:16	Sparse	12.06

In the post-processing of the collected radar images from ESA, first the product header files and then the image DN values are extracted and are geo-coded by using 1/25000 and 1/100000 scaled topographic maps of the region.

Two incidence angle maps are computed for each radar image: *incidence angle* and *local incidence angle*. The former one, *incidence angle*, is computed for the whole swath (100 – 105 km) of SAR/ASAR image and by assuming a flat terrain for the area. It is the incidence angle utilized in the derivation of backscatter values. The latter one, *local incidence angle*, is computed for the study catchment area. The incidence angle grids are computed separately for the SAR and ASAR images of the same dates: 09-Oct-2004, 18-Dec-2004, 07-May-2005 and 20-Aug-2005, with the same resolution of the actual images, 12.5 m.

In the computation of the *local incidence angle* (θ_L) of the Kurukavak basin, topographic characteristics of the study area are utilized. For this purpose, first the slope and aspect maps of the basin are derived from Digital Elevation Model (DEM) of the catchment. The schematic representation of the Equation 2 [17], which is then used to compute the local incidence angle (θ_L), as presented in Figure 5.

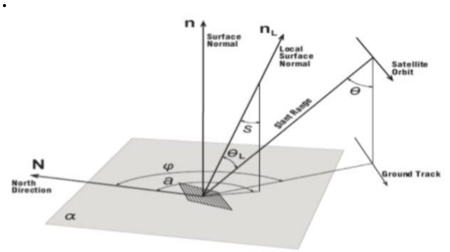

Fig. 5. The schematic representation of the parameters used for the local incidence angle (θ_L)

Similar to the computation of incidence angle grids, local incidence angle grids are calculated separately for the SAR and ASAR images of the dates: 09-Oct-2004, 18-Dec-2004, 07-May-2005 and 20-Aug-2005. Since the computation requires topography, these grids are evaluated within the basin boundary and with the same resolution of Kurukavak DEM, 30 meters.

$$\cos \theta_L = \cos(s) \times \cos(\alpha) + \sin(s) \times \sin(\alpha) \times \cos(\varphi - a) \quad (2)$$

where:

s is surface slope (radians)

a is surface aspect (radians, with geometric north equal to 0)

α is incidence angle (computed for GEM6 ellipsoid)

φ is flight track angle: angle between the satellite track and the geometric north (radians: obtained from product header file)

Similar to the derivation of incidence angle grids, backscatter values are computed for the whole swath width of the radar imagery as discussed by [9] and [13]. The backscatter values are derived in amplitude first and then they are converted to decibel (dB) units for analysis of radar images.

5. RESULTS AND DISCUSSION

5.1-Radar backscatter and surface roughness for various land covers

One of the major goals of this study is to establish an accurate relationship between radar backscatter and surface roughness for various land covers (bare, sparsely vegetated areas and forest) of the basin. A semi-empirical backscatter model, Dubois Model, is utilized for the SAR and ASAR images of 09-Oct-2004, 18-Dec-2004 and 20-Aug-2005 dates.

This procedure is used to compute roughness values of the 126 point soil moisture measurement locations which are already shown in early sections. Since, three field study dates are considered, a total of 378 roughness values are obtained. In order to verify the accuracy of the applied procedure, two roughness values are computed for each point; one from the SAR and the other one from the ASAR images.

In the analysis of the calculated roughness values from both of the data sets, a procedure including two levels of reduction is carried out for eliminating some of the computed values. The first level of reduction is based on the Dubois model limitations and the second level is based on the assumption that SAR and ASAR datasets result in similar roughness values for the same locations. Then, the total number of points is reduced from 378 to 258 with the two levels of reduction procedure, an arithmetic average roughness value is computed for each point from Data Set I for SAR and Data Set II for ASAR separately for the derivation of backscatter (SAR & ASAR) versus soil surface roughness relationship as presented in Figures 6 a&b. . Similar relationships are also developed by [10] and [20]. Moreover, since both the SAR and ASAR images are acquired with a 5.3 GHz frequency and have similar incidence angles, the computed regression equations were almost identical.

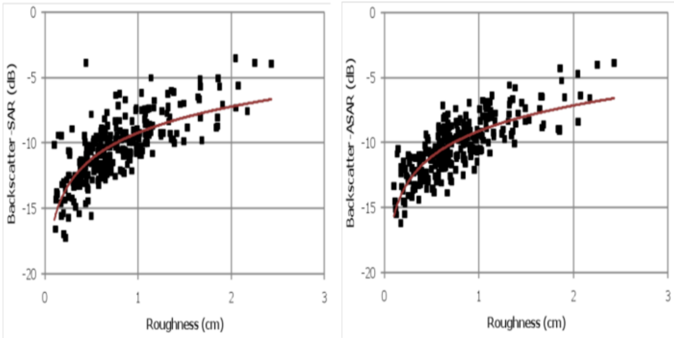

Fig. 6. a,b Backscatter versus soil surface roughness relationship for two data sets

5.2-Mapping of Surface Soil Moisture distribution using three methods

The distributed surface soil moisture maps of the basin are obtained to be used as an input to a hydrological model. This is achieved for the four field study dates of 09-Oct-2004, 18-Dec-2004, 07-May-2005 and 20-Aug-2005, and two soil moisture maps are obtained for each day, resulting from the SAR and ASAR image processing, respectively. The development and application steps of the three different methodologies are discussed below depending on the land use class and vegetation cover condition of the basin;

Method I – Backscatter Correction (BS) Factors, is used for the farmland and pasture fields of the basin for 09-Oct-2004, 18-Dec-2004, and 20-Aug-2005 dates when these areas have almost no vegetation cover. First, a nonlinear model relating radar backscatter with roughness, moisture and local incidence angle is developed with the point soil moisture measurements, which is then used to compute backscatter correction factors that are applied to the other farmland and pasture fields of the basin.

Method II – Water Cloud Model (WCM), proposed and applied by [1] and [18], a rather simple approach for modeling of backscatter from a vegetation canopy, known as the Water Cloud Model (WCM). This method is used for the farmland and pasture fields of the basin for 07-May-2005 when these areas are under dense vegetation cover. In this method, a semi-empirical backscatter model, the Water Cloud Model, is used in conjunction with the relationships developed for the first methodology. Basic assumptions of this model are described by [18] and [3].

Method III – Basin Indexes (BI), is used for the forested areas of the basin for the field study dates of 09-Oct-2004, 18-Dec-2004, 07-May-2005 and 20-Aug-2005. Since radar waves could not penetrate through dense forest cover, radar images are impractical for moisture estimation in these areas. Hence, topographic index and solar radiation index of the basin are used to develop a relationship between soil moisture and these two basin indexes. The most commonly used terrain index is the topographic wetness index, proposed by [2].

For these three methods discussed for soil moisture estimation, only Method II-WCM depends on vegetation by means of normalized difference vegetation index (NDVI). However, it is also found out that the land use class (farm or pasture) has no significant effect on the vegetation parameters of the WCM. As a result, land use classes of the basin are grouped under two major classes; i) Forest and Other, ii) Farmland and Pasture, for surface soil moisture mapping.

In the computation of surface soil moisture values of the Kurukavak catchment, the aforementioned three methods are re-used depending on the land use class and vegetation cover conditions of the area, and summarized in Table IV. Moreover, computation of surface roughness values for the farmland and pasture areas of the basin; for 09-Oct-2004, 18-Dec-2004, 07-May-2005 and 20-Aug-2005 field study dates is also determined in similar way using method I to III.

TABLE IV
Summary of the application of the soil moisture estimation methods

Date	Farmland & Pasture	Forest & Other
09-Oct-2004	Method I *Backscatter(BS) Correction*	Method III *Basin Indexes*
18-Dec-2004	Method I *BS Correction*	Method III *Basin Indexes*
07-May-2005	Method II *WCM*	Method III *Basin Indexes*
20-Aug-2005	Method I *BS Correction*	Method III *Basin Indexes*

The estimated surface soil moisture distributions of the Kurukavak catchment are presented in Figures 7a, b as an example for 09-Oct-2004, field study date both for the SAR and ASAR images. The volumetric soil moisture values (m_v values) are given in $m^3\ m^{-3}$ units (on a range from 0 to 1), but in order to have better representation in mapping of soil moisture, these values are multiplied by 100 and given in units of *percentages (%)* which is on a range from 0 to 100. The statistical parameters; such as mean, standard deviation etc., of the volumetric soil moisture distributions are calculated for:

a) The entire basin soil moisture distribution map using both methods I and III,

b) The farmland and pasture fields of the basin,

where soil moisture values are calculated with Method I (BS) and method II (WCM),

c) The forest and other land use types, where soil moisture values are computed with Method III (BI).

They are compared with the observed soil moisture measurements recorded on the same day (in %) from the field visits as shown in Table V. The mean soil moisture values ranged from 16.52 % for the field observations to 21 % resulted from SAR and from ASAR images for the processed date, 09 October 2004.

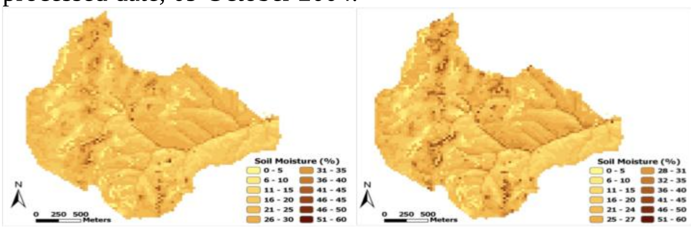

Fig. 7. a,b Soil moisture distribution maps of the basin using SAR and ASAR for 09-Oct-2004

TABLE V
Statistical parameters of the computed and observed volumetric soil moisture values for 09-Oct-2004

		09-Oct-2004 SAR (%)	09-Oct-2004 ASAR (%)
Entire Basin Methods I and III *(n = 5258)*	*Mean*	20.93	21.00
	Std. Dev.	6.57	6.57
	Max	47.09	48.33
	Min	0.02	0.04
Farmland and Pasture Method I *(n = 2392)*	*Mean*	20.57	20.73
	Std. Dev.	8.31	8.38
	Max	47.09	48.33
	Min	0.02	0.04
Forest and Other Method III *(n = 2866)*	*Mean*	21.17	21.18
	Std. Dev.	5.06	5.04
	Max	36.80	36.80
	Min	4.33	4.33
Point Soil Moisture Measurements *(n = 126)*	*Mean*	16.52	
	Std. Dev.	5.27	
	Max	31.27	
	Min	7.04	

5.3- Hydrologic model simulations

Hydrologic Engineering Center–Hydrologic Modeling System [7] is selected for simulation studies. This system is designed to simulate the precipitation-runoff processes of watershed modeling. The flood event on 1-Jun-2005 is selected for simulation with the HMS model by considering a time window of one month.

Initial deficit is the only model input parameter that differs among the simulations. The model parameters used in the HMS event simulations is determined first (see reference). In addition, numerical values such as peak flow, time of peak flow, total flow etc. which are representing the computed flow hydrographs are computed for presentation in Table VI. The percent change between the total flows and peak flows of the observed and simulated hydrographs are also shown using the calculated root mean square errors (RMSE) between the computed and observed flow values. Lastly, graphical outputs of the simulation runs are presented in Figures 8 a, b and c. The RMSE value of the distributed SAR and distributed ASAR simulations are both gave a value of 0.35. On the other hand, the same value is computed as 0.43 for the Lumped model simulation.

TABLE VI
Comparison of simulation model results with the observed hydrograph values

	Observed	Model Simulations		
		Lumped	Distributed SAR	Distributed ASAR
Peak Discharge (m^3/s)	9.97	10.89	9.77	9.90
Time of Peak(date-hr:min)	1-Jun-2005 07:20	1-Jun-2005 07:20	1-Jun-2005 07:20	1-Jun-2005 07:20
Total Flow (x 1000 m^3)	118.10	118.29	109.23	109.89
Difference in Peak Flows (%)		9.2	2.0	0.7
Difference in Total Flows (%)		0.2	7.5	7.0
Root mean square error (RMSE)		0.43	*0.35*	0.35
Figure Number		8a	8b	8c

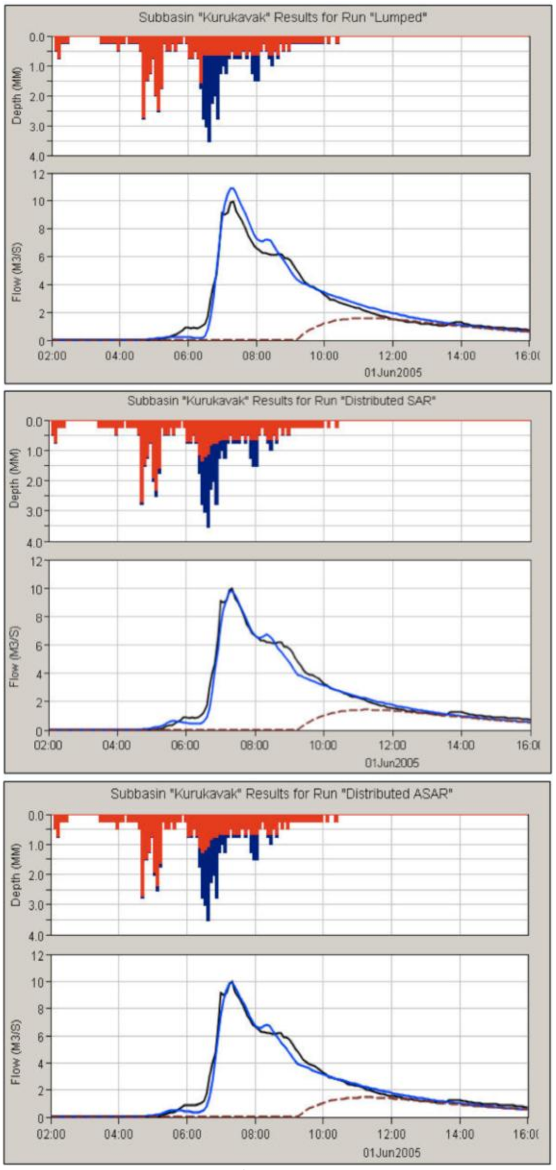

Fig. 8. a,b and c Results of the lump and distributed *SAR/ASAR* model runs for 01 June 2005

6. CONCLUSIONS

Soil moisture is an important variable that controls various land surface processes and it is essential component to weather forecasting, climate modeling and flood simulation studies. In spite of its importance to several disciplines, areal soil moisture information is not widely available on watershed and regional scales to be introduced for model runs. Consequently, development of better estimation techniques for soil moisture, especially with the integration of remote sensing imagery, is a challenging but promising field of investigation in hydrologic model studies.

The main objective of this study is to derive areal soil moisture information from active microwave remote sensing which is achieved through development and application of various methodologies using recent techniques. In this respect, a micro catchment in western Anatolia is selected as a case study, and a number of studies in the field are carried out for collection of point soil moisture data. In addition, active microwave images of the basin for these dates are also acquired from European Space Agency (ESA) and processed.

As a fist step, a methodology for soil roughness mapping of the study basin is followed, with the inversion of the Dubois backscatter model. Despite the fact that this method is successfully applied to the bare or sparsely vegetated surfaces of the basin, it has limitations from both the Dubois model and initial assumption of the applied technique. As a result, surfaces from smooth to medium level of roughness can only be extracted from remote sensing data.

The second methodology is applied to develop an algorithm for reliable estimation of soil moisture from radar imagery on bare or sparsely vegetated surface conditions. In this respect, the wet soil backscatter relationship is developed and further used within the soil moisture estimation methods. A variation of this relationship is utilized within the Backscatter Correction Factors method, which is the first method used for producing soil moisture maps of the study catchment. Both of the developed backscatter relationships and the applied method are found very promising that they could be easily implemented for future studies.

Extracting soil moisture distribution of the study basin under dense vegetation cover condition is the third step which is discussed in the main text. It is accomplished with an implementation of delta index algorithm with the Water Cloud Model, which is also the second method used for soil moisture mapping of the Kurukavak catchment. Even if the outcomes of this technique are found to be relatively successful, it has certain drawbacks due to the limitations of the Water Cloud Model in describing the complexity of the actual physical condition. Basin Indexes method is used for soil moisture mapping of the Kurukavak basin for the forested areas. Topographic and solar radiation indexes are utilized to build a linear relationship between these watershed indexes and point soil moisture measurements. The linear relationship is then applied to the forest land use class of the catchment, where microwave remote sensing of soil parameters is not possible. Since the method is solely developed on terrain indexes, the relationship is independent of land use conditions. It should be noted that this method has a general tendency to overestimate dry soil condition and underestimate the wet soil condition.

Soil moisture maps of the whole basin are finally produced for four selected days with the three methods; Backscatter Correction Factors method is applied for bare or sparsely vegetated, Water Cloud Model is used for densely vegetated and Basin Indexes method is applied for forested land use conditions of the watershed.

In the last part of the paper, the computed soil moisture distribution maps are introduced as an input to a semi-distributed hydrological model for the simulated flood event and compared with the simulation results performed with the lumped initial moisture condition. A major difference in the decay of computed infiltration rates is observed between these conditions. Even if a constant value is defined for the model, an exponential decay in the infiltration rate, which is similar to the actual behavior, is observed for the distributed condition. The RMSE value of the distributed SAR and distributed ASAR simulations are both obtained as 0.35; the same error value is found as 0.43 for the lumped model simulation. The differences in peak runoff records in percentages are ranged between 1-2 % for the distributed case and increased to 9% for the lumped model approach. But the runoff volume differences were found in reverse order being less as 0.2% for the lumped and increased to 7.5-7.0% for distributed model applications using MW radar images.

ACKNOWLEDGEMENT

This research is financially supported by the Scientific and Technological Research Council of Turkey (TUBITAK)-ÇAYDAG by two projects 104Y045-1001 and 107Y341_1002. The MW images are provided by the European Space Agency (ESA) through the joint collaboration between ESA and TUBITAK.

REFERENCES

[1] Attema, E.P.W., Ulaby, F.T., 1978, Vegetation Modeled as a Water Cloud, Radio Science, 19, 357 – 364.

[2] Beven, K.J., Kirkby, M.J., 1979, A Physically Based Variable Contributing Area Model of Basin Hydrology, Hydrology Science Bulletin, 24, 1, 43 – 69.

[3] Bindlish, R., Barros, A.P., 2001, Parameterization of Vegetation Backscatter in Radar-Based Soil Moisture Estimation, Remote Sensing of Environment, 76, 130 – 137

[4] Dubois, P., Van Zyl, J., Engman, T., 1995, Measuring soil moisture with imaging radars. IEEE Transactions on Geoscience and Remote Sensing, 33, 4, 915 – 926.

[5] Haider,S.S., Said,S., Kothyari,V.C., and Arora,M.K., 2004, Soil misture estimation using ERS2 SAR data: A case study in the Solani River catchmnet. Hydrological Sciences, 49,2, 323-334.

[6] Hain,C.R., Crow,W.T., Mecikalski,J.R., Anderson,M.C., and Holmes,T.,2011, An intercomparison of available soil moisture estimates from thermal infrared and passive microwave remote sensing and land surface modeling. J.of Geophyscical Research, 116, DOI:10.1029/2011JD015633.

[7] HEC, 2008, HEC-HMS version 3.2: User's Manuel, US Army Corps of Engineers Hydrologic Engineering Center, Davis, CA, USA.

[8] Hegarat-Mascle, S.Le., Zribi,M., 2002, Soil moisture estimation from ERS/SAR data. Toward an operational Methodology. IEEE Trans. on Geoscience and Remote Sensing, 40, 12.

[9] Laur, H., Bally, P., Meadows, P., Sanchez, J., Schaettler, B., Lopinto, E., Esteban, D., 2004, Derivation of the Backscatter Coefficient in ESA ERS SAR Products, European Space Agency, Technical Note, ES-TN-RS-PM-HL09, Issue 2, Rev. 5f.

[10] Leconte, R., Brissette, F., Galarneau, M., Rousselle, J., 2004, Mapping Near-Surface Soil Moisture with RADARSAT-1 Synthetic Aperture Radar Data, Water Resources Research, 40.

[11] Lilesand, T.M., Kiefer, R.W., 1999, Remote Sensing and Image Interpretation, John Wiley & Sons, New York.

[12] Parajka, J., Naeimi, V., Blöschl, G., Wagner, W., Merz, R., and Scipal,K., 2006, Assimilating scatterometer soil moisture data into conceptual hydrologic models at the regional scale. Hydrol. Earth Syst. Sci., 10, 353-368.

[13] Rosich, B., Meadows, P., 2004, Absolute Calibration of ASAR Level 1 Products Generated with PF - ASAR, European Space Agency, Technical Note, ENVI-CLVL-EOPG-TN-03-0010, Issue 1, Rev. 5.

[14] Rüdiger, C., Calvet,J.C., Gruhier,C., Holmes,T.H.R., De Jue, R.A.M., 2009, An intercomparison of ERS-Scat and AMRS-E soil moisture observations with model simulations over France. Journal of Hydrometeorology, 10, DOI:10.1175/2008JHM997.1, 431-447.

[15] Sahebi, M.R., Angles, J., Bonn, F., 2002, A Comparison of Multi-Polarization and Multi-Angular Approaches for Estimating Bare Soil Surface Roughness from Spaceborne Radar Data, Canadian Journal Of Remote Sensing, 28, 5, 641 – 662.

[16] Stein, M.L., 1999, Interpolation of Spatial Data: Some Theory for Kriging, Springer, New York.

[17] Su, Z., Troch, P.A., De Troch, F.P., 1997, Remote Sensing of Bare Soil Moisture Using EMAC/ESAR Data, International Journal of Remote Sensing, 18, 10, 2105 – 2124.

[18] Ulaby, F.T., Moore, R.K., Fung, A.K., 1981b, Microwave Remote Sensing Active and Passive, Volume II: Radar Remote Sensing and Surface Scattering and Emission Theory, Norwood, MA, USA.

[19] Weismann, A., Schonermark, M.V., Schumann, A., Jorn, P., and Günter, R., 1998, Soil moisture estimation with ERS-1 SAR data in the East-German loess soil area. Int. J. of Remote Sensing, 19, 2, 237-243.

[20] Zribi, M., Dechambre, M., 2002, A New Empirical Model to Retrieve Soil Moisture and Roughness from C-Band Radar Data, Remote Sensing of Environment, 84, 42 – 52.